RNA-TorsionBERT: leveraging language models for RNA 3D torsion angles prediction

Clément Bernard[1,2], Guillaume Postic[1], Sahar Ghannay[2], and Fariza Tahi[1]

[1]Université Paris Saclay, Univ Evry, IBISC, 91020, Evry-Courcouronnes, France

[2]LISN - CNRS/Université Paris-Saclay, France, 91400, Orsay, France

Predicting the 3D structure of RNA is an ongoing challenge that has yet to be completely addressed despite continuous advancements. RNA 3D structures rely on distances between residues and base interactions but also backbone torsional angles. Knowing the torsional angles for each residue could help reconstruct its global folding, which is what we tackle in this work. This paper presents a novel approach for directly predicting RNA torsional angles from raw sequence data. Our method draws inspiration from the successful application of language models in various domains and adapts them to RNA. We have developed a language-based model, RNA-TorsionBERT, incorporating better sequential interactions for predicting RNA torsional and pseudo-torsional angles from the sequence only. Through extensive benchmarking, we demonstrate that our method improves the prediction of torsional angles compared to state-of-the-art methods. In addition, by using our predictive model, we have inferred a torsion angle-dependent scoring function, called RNA-Torsion-A, that replaces the true reference angles by our model prediction. We show that it accurately evaluates the quality of near-native predicted structures, in terms of RNA backbone torsion and pseudo-torsion angle values. Our work demonstrates promising results, suggesting the potential utility of language models in advancing RNA 3D structure prediction.

The source code is freely available on the EvryRNA platform: https://evryrna.ibisc.univ-evry.fr/evryrna/RNA-TorsionBERT.

RNA 3D structure | Torsional angles | Language models | Scoring function

Correspondence: ***fariza.tahi@univ-evry.fr***

1. Introduction

RNA is a macromolecule that plays various biological functions in organisms. Similarly to proteins, the biological function of an RNA may be directly linked to its 3D structure. Experimental methods such as NMR, X-ray crystallography, or cryo-EM (1) can determine the 3D structure of RNAs, but they remain tedious in cost and time. Computational methods have been developed for predicting the 3D structure from the sequence, with three different approaches: *ab initio*, template-based and deep learning-based (2). Currently, no existing method matches the performance of AlphaFold 2 for proteins (3), as shown with the last results on the CASP-RNA challenge (4). Reaching AlphaFold's (3) level of accuracy is a long shot, notably due to the lack of data (5). Very recently, the release of AlphaFold 3 (6) has extended its predictions to a wide range of molecules like DNA, ligand, ion and RNA, but the results remain limited for RNA (6, 7).

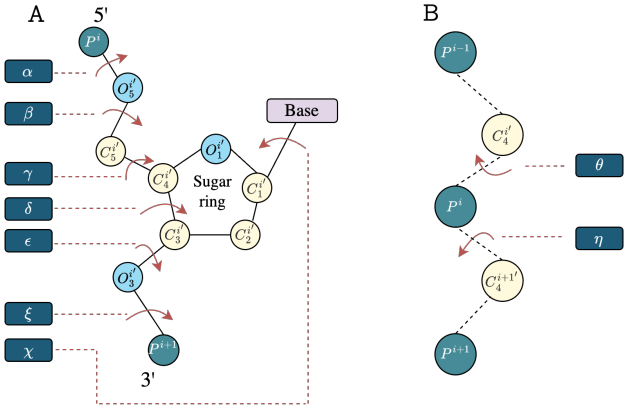

Figure 1. The seven RNA torsional angles and the two pseudo-torsional angles. (A) RNA backbone torsional angles. The angles are defined around $O3'_{i-1}/P_i/O5'_i/C5'_i$ (α), $P_i/O5'_i/C5'_i/C4'_i$ (β), $O5'_i/C5'_i/C4'_i/C3'_i$ (γ), $C5'_i/C4'_i/C3'_i/O3'_i$ (δ), $C4'_i/C3'_i/O3'_i/P_{i+1}$ (ϵ), $C3'_i/O3'_i/P_{i+1}/O5'_{i+1}$ (ζ) and the rotation of the base relative to the sugar (χ) $O4'_i/C1'_i/N1_i/C2_i$ for pyrimidines and $O4'_i/C1'_i/N9_i/C4_i$ for purines. (B) RNA pseudo-torsional angles. η is defined around $C4'_{i-1}/P_i/C4'_i/P_{i+1}$ and θ around $P_i/C4'_i/P_{i+1}/C4'_{i+1}$.

RNA can adopt various secondary motifs, along with a wide range of complex interactions that contribute to its 3D structure. Research efforts have focused on classifying both the canonical and non-canonical pairs (8), further supported by the description of the backbone conformation (9, 10). Unlike proteins, RNA backbone structures are defined by seven torsional angles, the natural manifold of all these dihedral angles combined being a 7-dimensional hypertorus, which presents a significant challenge both statistically and computationally. Pyle and colleagues have shown that they can be approximated by two pseudo-torsional angles (see Figure 1) (11). Understanding these torsional angles is crucial for comprehending the 3D structures of RNA, which in turn could aid in predicting their folding, as done for proteins (12, 13).

Current predictive methods for RNA 3D structure prediction do not always integrate torsional angles, missing important features to comprehend its folding. To the best of our knowledge, only one work has been done to predict exclusively torsional angles from RNA sequence, SPOT-RNA-1D (14), using a residual convolutional neural network.

In this work, we aim to leverage language models to better apprehend the prediction of RNA torsional angles from its sequence. Indeed, works have been proposed through the years to work on biological sequences, inspired by the suc-

cess of language models like BERT (15). Its adaptation for RNA (16) or DNA (17, 18) shows promising results which could be leveraged for other RNA structural features prediction.

Another interest in torsional angles for RNA 3D structures is for quality assessment. Without the help of reference structures, scoring functions have been developed to assess structural quality. These methods can be knowledge-based (19–22) using statistical potentials or deep learning (23, 24). The knowledge-based scoring functions consider RNA structural features as inputs like pairwise distances (20, 21, 25) or with the help of torsional angles (19, 22). We propose here a new scoring function based on the extension of our model to predict RNA torsional angles. This scoring function allows us to assess structural quality in torsional angle space.

This paper is organized as follows: we describe our contributions in two separate points. Each section is divided into two parts: one for the work on torsional angle prediction and the other for our proposed scoring function. We detail our experiments for the torsional angles prediction and the structural quality assessment tasks before discussing our approaches' results and limitations. We then conclude by discussing the scope of our contributions. The results and the code of our RNA-TorsionBERT and RNA-Torsion-A are easily reproducible and freely available on the EvryRNA platform: https://evryrna.ibisc.univ-evry.fr/evryrna/RNA-TorsionBERT.

2. Methods

This section presents our model for predicting RNA torsional angles and then the scoring function derived from our model.

A. Torsional angles prediction

A.1. RNA-TorsionBERT approach. Current methods that use sequence as inputs for RNA-related approaches only represent sequences as one-hot-encoding vectors (26, 27). This representation may be too sparse to consider sequential interactions well. This encoding is usually associated with a convolutional neural network, which is commonly limited by long-range interactions. A solution could be using attention mechanisms (28). Attention-based architecture nonetheless requires a huge amount of data to train well, which is not the case for RNA 3D structure data. To counter this problem, we can use models pre-trained on a large amount of unlabeled data. This could bring a better input representation of the raw sequence, which could then be fine-tuned to specific tasks. These pre-trained models could input either RNA or DNA sequences. Indeed, the alphabet of DNA is nearly the same as RNA in terms of vocabulary, with only one nucleotide change: the T for DNA and the U for RNA. Their similarity in sequences could be leveraged into language-based models to create embeddings for RNA sequences. This could mitigate the lack of data from RNA and thus help a model start from an embedding that already has a meaning.

Recent advances in language models started with BERT (15), where the model was pre-trained on masking and next-sentence prediction tasks before being fine-tuned on diverse specific language tasks. DNA or RNA can be seen as a sequence of nucleotides, where their interactions have a biological meaning. Therefore, methods have been adapted from BERT to develop a language-based architecture for either RNA or DNA. The aim is to reproduce the success of language comprehension for another language. As the size of the vocabulary is different, modifications should be made to fit the current language. An example for DNA is DNABERT (17), where the training process was updated compared to the original BERT by removing the next sentence prediction and taking K-mers as inputs (contiguous sequence of k nucleotides). It was trained on human-genome data. Its second version, named DNABERT 2 (18), uses Byte Pair Encoding (BPE) instead of K-mers. An example of adaptation of BERT for RNA is called RNABERT (16). It is a six-transformer layer pre-trained on two tasks: masking and structural alignment learning (SAL). RNABERT was trained on 76,237 human-derived small ncRNAs. Other methods have been adapted to RNA language but uses MSA as inputs like RNA-FM (29), Uni-RNA (30) or RNA-MSM (31). Nonetheless, they require multiple sequence alignment (MSA) as inputs, which restricts the use for RNAs. Indeed, there are a numerous amount of unknown structures (32), and MSA will restrict the adaptation to future unseen families. In this article, we decided to only consider sequences as inputs, and so for the language models.

The aim of our method is, given a pre-trained language model (DNABERT or RNABERT), to adapt its neuronal weights to predict RNA torsional and pseudo-torsional angles from the sequence. We have added layers to adapt the methods to our multi-token label regression task. Each token in the input would have 18 labels: two values (sine and cosine) for each of the seven torsional angles and two pseudo-torsional angles. The use of pre-trained embedding would help the model not to start from scratch and update the learned attention layers for RNA structural features.

A.2. RNA-TorsionBERT architecture. The architecture of our method, when based on DNABERT, is described in Figure 2 (illustrated with 3-mers). An input sequence of size L is tokenized and then fed to the network with token and positional embeddings. The tokenization process usually adds specific tokens (like the *CLS* and *PAD* tokens). As DNABERT could input a maximum of 512 tokens, we set the maximum sequence length to 512 nucleotides. The last hidden state is set to be 768 by the original DNABERT architecture. We then apply extra layers to map the hidden state outputs to the desired final output dimension (Lx18). These extra layers comprise layer normalisation, a linear layer (from 768 to 1024), a GELU activation, another linear layer (1024 to 18), and a Tanh final activation. The final output layer is of size 18 because it outputs a sine and a cosine for the seven and two pseudo-torsional angles. It allows the relief of the periodicity of the different angles. The Tanh activation maps the outputs to the cosine and sine range (between -1 and +1), which is then converted into angle predictions using the formula $\alpha = \tan^{-1}(\frac{\sin(\alpha)}{\cos(\alpha)})$ (adaptable for the other angles). Details

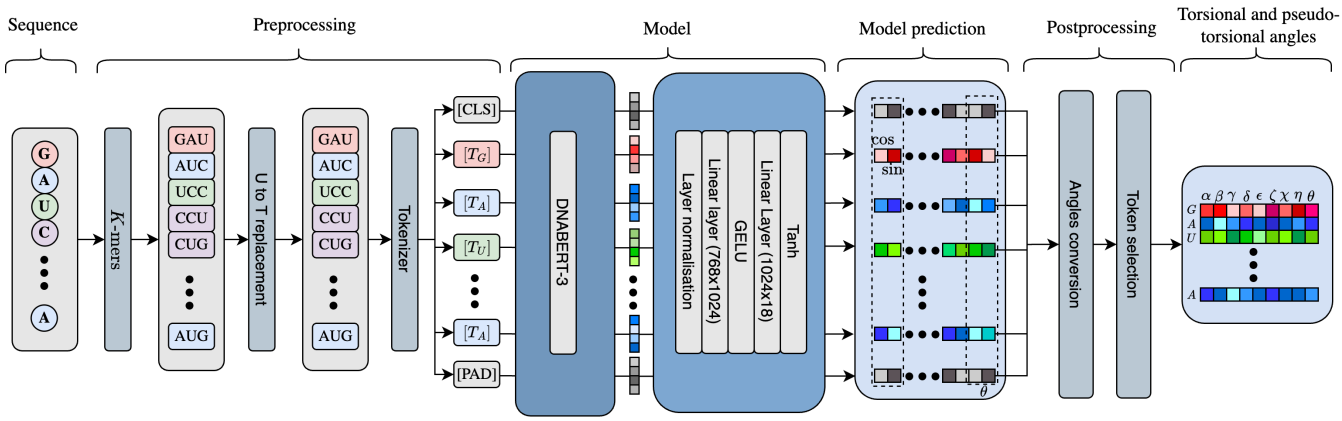

Figure 2. Schema of the proposed language model architecture for torsional and pseudo-torsional angles prediction. Given an RNA sequence, preprocessing is applied to map each sequence's nucleotide into a token with pre-trained embeddings from the language model. *CLS* and *PAD* tokens are added to the sequence tokens. We convert the Uracil (U) with its equivalent in DNA: Thymine (T) for DNABERT model. Then, the language model (DNABERT or RNABERT) will output hidden states with a representation of each token. This is fed into extra layers before entering a last Tanh activation to have the cosine and sine per angle. A postprocessing is required to convert back to angles from the sine and cosine.

on the training process are in the Supplementary file.

B. Model quality assessment based on torsional angles

B.1. RNA-Torsion-A approach. The metric assessment of RNA 3D structures requires two structures, with one being the experimentally solved structure. Having this reference is a strong asset that can not be available when developing prediction models. To rank near-native structures without a reference, scoring functions have been developed throughout the years, adapting free-energy (19–22, 25). Other methods employ deep learning approaches like RNA3DCNN (23) or ARES (24).

To discriminate near-native structures in the torsional and pseudo-torsional space, we have derived a scoring function from our RNA-TorsionBERT model. We first have proven that the evaluation criteria used in RNA-TorsionBERT, the MAE (mean average error), has a high correlation with existing metrics. Then, we replaced the true torsional angles with the predicted angles from our model to compute the mean average error (MAE) over the near-native structure. Therefore, the MAE computation compares the prediction of our model angles with the angles from the predicted non-native structures. We named this scoring function RNA-Torsion-A (RNA torsional assessment).

In SPOT-RNA-1D (14), the authors introduced the mean-average error (MAE) metric to assess the performance of their method SPOT-RNA-1D in the prediction of torsional and pseudo-torsional angles. Given a sequence S of L residues and one angle $z \in Z = \{\alpha, \beta, \gamma, \delta, \zeta, \chi, \theta, \eta\}$, the MAE is computed as

$$\text{MAE(z)} = \min(d_z, 360 - d_z)$$

with:

$$d_z = \frac{1}{L} \sum_{res \in S} |z_{res}^{pred} - z_{res}^{true}|$$

The angle z_{res}^{pred} defines the predicted angle computed for the nucleotide res of the sequence S. The angle z_{res}^{true} corresponds to the angle of nucleotide res experimentally determined. While it has only been considered angle per angle in SPOT-RNA-1D, we can extend this MAE by averaging the value over the different torsional and pseudo-torsional angles.

$$\textbf{MAE} = \frac{1}{|Z|} \sum_{z \in Z} \text{MAE(z)}$$

This formulation enables the computation of a unique value for two structures given their torsional angles. As it provides a quality score for two structures, it can be seen as a metric for RNA 3D structure quality assessment.

B.2. RNA-Torsion-A architecture. RNA structural quality is evaluated from features inferred from the RNA 3D structure, like base distances, chemical properties or even torsional angles. In knowledge-based approaches (19–22), these features can be used to compare the statistical potentials from a reference state (a state without RNA folding).

To compute RNA structural quality, we can consider our RNA-TorsionBERT predictions as the ground truth regarding angles and then compute the deviation from inferred angles from a candidate structure. Therefore, if we use the inferred angles from the candidate structure, the MAE with the predicted angles from our RNA-TorsionBERT model (given the sequence of the structure) will give a quality score. This MAE now becomes a scoring function, as it only takes as input a structure without any known native structure. Figure 3 shows the architecture of our scoring function. We used the DSSR (33) tool, which is a software to infer torsional angles from the structures. Given a structure, the DSSR (33) outputs the inferred torsional angles and the sequence. The sequence is then pre-processed by RNA-TorsionBERT, and the inference gives predicted angles. Then, we compute the MAE to finally output a structural quality measure for an RNA 3D structure.

The MAE is therefore extended to be a scoring function but can also be a metric for RNA structural assessment. In-

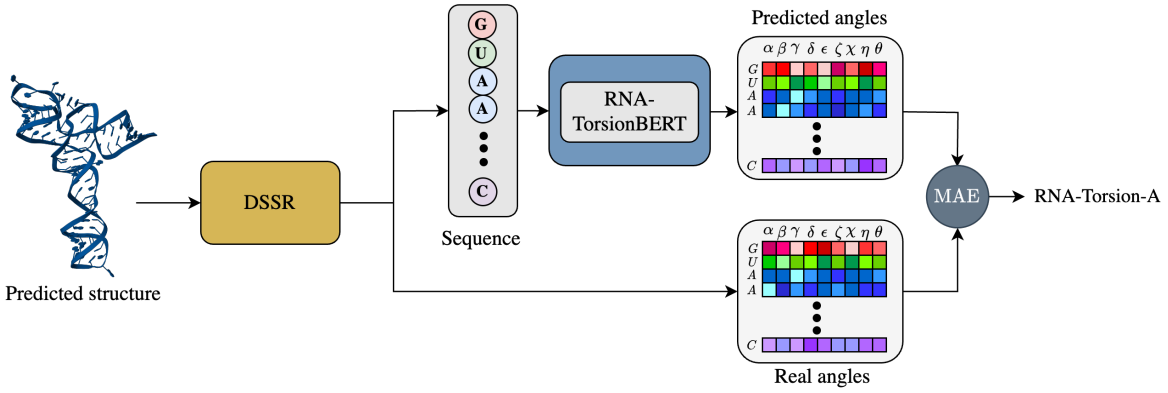

Figure 3. RNA-Torsion-A scoring function computation. Given a predicted RNA 3D structure, the DSSR (33) software gives the sequence and calculates angles. The sequence is fed to our RNA-TorsionBERT model to predict the different angles. The scoring function is then computed by taking the MAE between the predicted angles and the angles read from the RNA 3D structure.

deed, given two structures, the MAE computed on inferred angles from the candidate and the reference gives a quality score to assess RNA structural quality. Schema of the MAE as a metric is displayed in Figure S3 of the Supplementary file.

3. Results and Discussion

A. Results on Torsional Angles prediction

We present here the different experiments for the torsional angles prediction task. We used the MAE presented above as a criterion to assess our model performances.

A.1. Datasets. To validate the performances of torsional angle prediction models, we used different datasets of native structures:

Pre-training: we downloaded each available PDB structure and removed the structures from the non-redundant Training, Validation and Test sets presented below. We also ensure the structures from this dataset have a sequence similarity below 80% compared to the other used datasets. This dataset aims to give an overall idea of the native structures and is then used to pre-train our language models. We considered only the structures of a maximum sequence length of 512 (DNABERT can only input 512 tokens). The final set is composed of 4,267 structures with sequences from 11 to 508 nucleotides.

Training: we used the training set from rsRNASP (22). It is composed of 185 3D structures with sequences between 17 and 395 nucleotides.

Validation: we used the validation structures from SPOT-RNA-1D (14). It contains 29 structures with sequences between 33 and 288 nucleotides.

Test: we combined two well-known test sets: RNA-Puzzles (34–37) and CASP-RNA (4). We combined both of these datasets as a whole Test set to assess the robustness of our model. It leads to a Test set of 52 structures (40 from RNA-Puzzles and 12 from CASP-RNA), with sequences from 27 nucleotides to 374 (we remove the RNA of PDB ID R1138 as its length exceeds 512 nucleotides).

The distribution of the seven torsional angles and the two pseudo-torsional angles is given in Figure 4. These distributions are similar for the four datasets, meaning the learned distribution from the training set could allow good generalisation for the model.

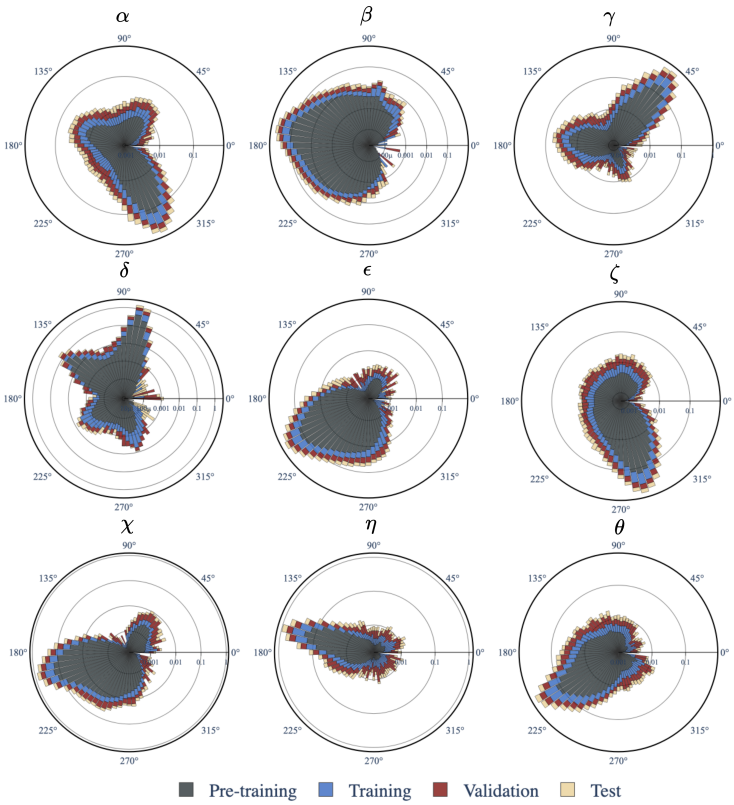

Figure 4. Polar distribution of the seven torsional angles ($\alpha, \beta, \gamma, \delta, \epsilon, \zeta, \chi$) and the two pseudo-torsional angles (η and θ) for the Pre-training, Training, Validation and Test datasets. For each angle, the logarithm of the normalized count is depicted.

Table 1. MAE (in °) for the Validation set averaged for the nine angles for DNABERT (3,4, 5 or 6-mers) and RNABERT. The 3-mer (pre) is DNABERT with 3-mer trained over the Pre-training dataset before being fine-tuned to the Training set. We did it only for DNABERT 3-mer as it was the model with the best mean MAE.

RNABERT	DNABERT					
	-	3-mer	4-mer	5-mer	6-mer	3-mer (pre)
α	48.8	**43.4**	43.6	46.7	47.7	46
β	**19.9**	21.0	22.6	22.3	22.9	20.8
χ	20.2	20.5	20.6	20.2	20.7	**19.6**
δ	18.7	17.4	16.7	17.0	17.0	**16.2**
ϵ	**19.5**	19.7	19.9	20.5	22.5	19.7
η	27.4	27.2	28.1	26.8	27.6	**25.4**
γ	35.8	34.6	36.7	36.2	36.2	**34.5**
θ	30.5	32.6	32.1	29.9	31.5	**29.5**
ζ	33.8	33.1	33.5	32.7	34.8	**31.7**
Mean	28.3	27.7	28.2	28.1	28.9	**27.1**

A.2. Language model selection. Each language model has a different format of inputs (K-mers for DNABERT and single nucleotides for RNABERT), we had to select the best tokenization of our RNA sequences. We also had to decide which pre-trained model was the best for our task. Therefore, we trained the same DNABERT model with the different values of K (3, 4, 5 or 6) and RNABERT on the Training set and observed the performances on the Validation set. We did not use DNABERT 2 because the inputs are encoded with byte pair encoding; It loses the nucleotide level representation, and thus, we can not predict torsional angles for each nucleotide.

The results are shown in Table 1 on the validation set. In terms of K-mers, DNABERT trained on 3-mers has better results (averaged MAE of 27.7°) than the other K-mers and RNABERT, even if it does not outperform them for each torsional angle.

DNABERT with 3-mers outperforms RNABERT, which does not input K-mers. This result remains surprising as we could have thought that RNABERT, as pre-trained specifically on RNA data, could have done better than the DNABERT model. This difference might be explained by the K-mers representation that is used by DNABERT compared to RNABERT, where the size of the vocabulary is extended, and thus a finer representation of the inputs is embedded. It could also be explained by the larger number of pretrained sequences that allow to have a finer embedding of nucleotide sequences.

We improved these results by pre-training the best model from these results, DNABERT with 3-mers, on the Pre-trained dataset before fine-tuning it on the Training set. It led to an MAE of 27.1, a mean improvement of 0.6°.

For the rest of the article, we name RNA-TorsionBERT (for RNA torsional BERT) the DNABERT with 3-mers firstly trained on the Pre-training dataset and then fine-tuned on the Training dataset.

A.3. Performances. We present here the prediction results obtained by our method RNA-TorsionBERT on the Test set (presented above) compared to the state-of-the-art approach SPOT-RNA-1D (14), which is the only method that predicts RNA torsional angles from the sequence only. We reproduced the architecture of SPOT-RNA-1D (because we only had the code to do inference) and trained it with the exact same data as RNA-TorsionBERT. We also included the results for the inferred angles from methods benchmarked in State-of-the-RNArt (2). The methods included either *ab initio* with IsRNA (38) and RNAJP (39), or template-based with RNAComposer (41), Vfold-Pipeline (40), MC-Sym (42) and 3dRNA (43). We also include three deep learning methods: trRosettaRNA (44) and RhoFold (45) and the newly AlphaFold 3 (6).

We report the averaged angle MAE on the Test Set in Table 2. Details of the MAE for each angle and each structure are reported in Figure S1 of the Supplementary file.

Our RNA-TorsionBERT model has better performances than SPOT-RNA-1D for every angle. It has an average MAE on all angles of 22.6° compared to 30° for SPOT-RNA-1D. The MAE improvement ranges between 2.1° (for θ) and 14.7° (for δ). It also outperforms the angles inferred from state-of-the-art methods for RNA 3D structure prediction, including the last published method, AlphaFold 3 (6). AlphaFold 3 outperforms the other deep learning approaches for the inferred torsional angles but is beaten by an *ab initio* method (IsRNA1), SPOT-RNA-1D and our RNA-TorsionBERT approaches. trRosettaRNA and RhoFold, two deep learning methods, have the worst MAE compared to *ab initio* and template-based approaches. It can be explained by the use of physics in *ab initio* and template-based methods that are inferred in the torsional angles. The use of deep learning approaches might have the counterpart to not include physics enough, except for AlphaFold 3. Deep learning methods, while having the best overall results, as shown in the benchmark done in State-of-the-RNArt (2), remain limited in torsional angle predictions.

Figure 5 reports the MAE averaged over the nine angles obtained by our method and by SPOT-RNA-1D on each RNA of the Test set. We can see our method achieves more frequently MAE below 20° than SPOT-RNA-1D, and sometimes achieves MAE below 10° (which is not the case for SPOT-RNA-1D). For sequences higher than 230 nucleotides, our method seems similar to SPOT-RNA-1D.

Details on examples of structures with good and bad performances in terms of MAE from RNA-TorsionBERT are shown in Figure S1 of the Supplementary file. MAE values per angle for each RNA structure are displayed in Figure S2 of the Supplementary file.

B. Model quality assessment based on torsional angles

In this part, we describe the different datasets used for the evaluation of our scoring function. We used correlation scores to compare the performances and the links of our scoring function to existing metrics.

Table 2. MAE (in °) per angle averaged over the Test set for RNA-TorsionBERT compared to the state-of-the-art method SPOT-RNA-1D (14). We also include inferred torsional angles from state-of-the-art methods that predict RNA 3D structures. The MAE was computed for those methods only on single-stranded structures, as in State-of-the-RNArt (2). Methods are sorted by mean MAE.

	Method type	α	β	γ	δ	ϵ	ζ	χ	η	θ	Mean
RNA-TorsionBERT	Deep Learning	**37.3**	**19.6**	**29.4**	**13.6**	**16.6**	**26.6**	**14.7**	**20.1**	**25.4**	**22.6**
SPOT-RNA-1D (14)	Deep Learning	50.7	30.1	35.8	28.3	21.9	29.8	20.9	25.0	27.5	30.0
IsRNA1 (38)	*Ab initio*	53.1	26.2	39.2	14.6	25.9	38.4	19.0	27.6	31.7	30.6
AlphaFold 3 (6)	Deep Learning	51.2	26.5	38.0	17.0	21.3	38.3	20.5	30.2	36.3	31.0
RNAJP (39)	*Ab initio*	56.8	31.6	41.9	18.6	27.7	42.1	21.1	29.8	33.3	33.7
Vfold-Pipeline (40)	Template-based	55.4	28.1	38.8	20.1	32.2	43.1	25.0	34.2	41.5	35.4
RNAComposer (41)	Template-based	58.9	31.5	48.2	17.9	27.1	40.0	24.8	32.8	38.6	35.5
MC-Sym (42)	Template-based	72.2	31.2	61.5	31.8	25.6	49.4	29.6	41.2	44.6	43.0
3dRNA (43)	Template-based	65.7	40.0	53.6	33.7	40.3	52.7	27.2	40.2	45.6	44.3
trRosettaRNA (44)	Deep Learning	67.6	36.8	67.0	26.4	32.9	54.3	58.3	38.2	48.3	47.8
Rhofold (45)	Deep Learning	94.3	66.0	76.2	60.6	52.8	72.6	32.4	42.0	46.6	60.4

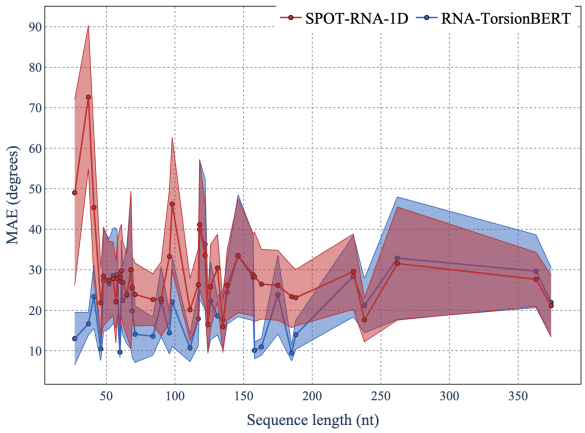

Figure 5. Mean MAE and standard deviation averaged over the angles depending on the sequence length of the RNAs from the Test set for RNA-TorsionBERT and SPOT-RNA-1D.

B.1. Datasets. Datasets of near-native structures (or decoys) are necessary to compare model quality assessment metrics. Indeed, scoring functions are used to discriminate between near-native structures, meaning that we need to have non-native structures to evaluate the quality of our scoring function.

We used three different datasets with different strategies of structure generation:

Decoy Test Set I is from RASP (20), composed of 85 native RNAs with decoys generated with MODELLER (20). MODELLER is a predictive model that is used to create decoys with different sets of Gaussian restraint parameters. Each RNA has 500 decoys, which are close to the native structure. We only kept 83 RNAs and removed the two RNAs that have sequence lengths higher than 512 nucleotides (PDB ID: 3df3A and 3f1hA).

Decoy Test Set II corresponds to the prediction-models (PM) subset from rsRNASP (22). It has 20 non-redundant single-stranded RNAs. For each RNA, 40 decoys are generated with four RNA 3D structure prediction models: FARFAR 2 (46), RNAComposer (41), SimRNA (47) and 3dRNAv2.0 (43). The decoys are not as near to native structures as with the Decoy Test Set I.

Decoy Test Set III is the RNA-Puzzles standardized dataset (48). This dataset comprises 21 RNAs and dozens of decoy structures for each RNA. The decoys are not all close to the native structures.

B.2. Evaluation measures. Scoring functions aim to discriminate near-native structures. The Pearson correlation coefficient (PCC) and the enrichment score (ES) are used to assess the correctness of a given scoring function. They assess the link between a scoring function and a given metric.

The Pearson coefficient correlation (PCC) is computed between the ranked structures based on scoring functions and structures ranked by metrics. It is defined as:

$$PCC = \frac{\sum_{i=1}^{N_{decoys}}(E_n - \bar{E})(R_n - \bar{R})}{\sqrt{\sum_{n=1}^{N_{decoys}}(E_n - \bar{E})^2}\sqrt{\sum_{n=1}^{N_{decoys}}(R_n - \bar{R})^2}}$$

where E_n is the energy of the nth structure, and R_n the metric of the nth structure. PCC ranges from 0 to 1, where a PCC of 1 means the relationship between metric and energy is completely linear.

The enrichment score (ES) considers top-ranked structures from both scoring function and metric. It is defined as:

$$ES = 100 \times \frac{|E_{top10\%} \cap R_{top10\%}|}{N_{decoys}}$$

where $|E_{top10\%} \cap R_{top10\%}|$ is the number of common structures from the top 10% of structures (measured by the metric) and the top 10% of structures with the lowest scoring function. ES ranges between 0 and 10 (perfect scoring). An enrichment score of 1 means a random prediction, whereas below 1 means a bad score.

B.3. MAE as model quality assessment. Existing metrics have been developed to assess the quality of predicted RNA 3D structures with access to a reference. The most famous one is the RMSD (root-mean-square deviation), which assesses the general folding of structures like ϵRMSD (25). ϵRMSD adds key RNA specifities to the RMSD computation. Protein-based approaches have also been adapted

to RNA, like the TM-score (49), which computes alignment and normalized distances. The GDT-TS (50) counts the number of overlaps for different thresholds, while the lDDT (51) assesses the interatomic distances. The CAD-score (52) evaluates the contact-area differences between two structures. More RNA-specific metrics have been introduced, like INF_{all} (53) (interaction network fidelity) that counts the number of key RNA interactions (Watson-Crick, non-Watson-Crick, stacking). It has been extended to the DI (53) (deformation index) with the incorporation of the RMSD. Finally, a torsional-angles-based metric, named MCQ (54) (mean of circular quantities), has been introduced. The MCQ computes the deviation in angle space with the superposition of structures and complements other existing metrics.

As recently done in RNAdvisor (55) where we benchmarked the existing scoring functions and metrics, we computed for the three Decoys sets the PCC and ES between nine existing metrics. To depict the legitimacy of the MAE as a model quality assessment, we added it as a metric to the previous ones. Results are shown in Figure 6 A).

We observe a correlation of 0.96 in terms of PCC between MAE and the MCQ, and an ES of 6.77. It means the MAE has a high correlation with the MCQ while having a lower correlation to other existing metrics (PCC below 0.7 and ES below 4.8 for the other metrics). It is the best PCC correlation over the existing metrics and one of the best in terms of ES. This means that the MAE could be a valuable metric compared to MCQ, and thus, it could be used to assess the quality of RNA 3D structures in terms of angle deviation and inspiring a scoring function.

B.4. RNA-Torsion-A as scoring function. To assess the validity of our scoring function, we computed with RNAdvisor (55) the available scoring functions RASP (20), ϵSCORE (25), DFIRE-RNA (21) and rsRNASP (22) for the three different Decoys test sets.

We compared RNA-Torsion-A with the state-of-the-art scoring functions using PCC and ES over nine metrics and the MAE. The averaged values are shown in Figure 6 B).
RNA-Torsion-A has a high correlation with MCQ and MAE (PCC/ES of 0.77/3.73 and 0.78/4.5, respectively, for MCQ and MAE), the highest compared to the other existing metrics. These results show that the RNA-Torsion-A scoring function correlates highly with MCQ (and MAE) compared to the other scoring functions. It reproduces quality assessment based on torsional and pseudo-torsional angles better than the other existing scoring functions. It is more linked to MCQ and MAE compared to rsRNASP (PCC of 0.77 for RNA-Torsion-A compared to 0.66 for rsRNASP with MCQ), which is the only state-of-the-art scoring function benchmarked that includes RNA torsional angles. Nonetheless, as shown in Figure 6 B), RNA-Torsion-A is not as correlated as the other scoring functions compared to the distance-based existing metrics (see more details in Figure S2 of the Supplementary file). Indeed, as it only considers the torsional features, our scoring function allows the comparison in angle space but does not enable atom distance consideration.

4. Conclusion

In this work, we have developed a language-based model, RNA-TorsionBERT, to predict RNA torsional and pseudo-torsional angles from the sequence. With a DNABERT 3-mers model, the learned embeddings have been used as a starting point to infer structural features from the sequence. We have achieved improvement compared to SPOT-RNA-1D (14), the only tool for RNA torsional angle prediction from the raw sequence.

Through an extensive benchmark of state-of-the-art methods, we have outperformed the angles inferred from the predictive models. We have also included in the benchmark the new release of AlphaFold, named AlphaFold 3 (6), which gives the best results compared to *ab initio*, template-based and deep learning solutions in terms of MAE on inferred angles. Our method, RNA-TorsionBERT, remains better for the prediction of RNA torsional angles with only the sequence as input, while AlphaFold 3 uses MSA as inputs.

Most protein methods or current deep learning methods (44, 57–60) for predicting RNA 3D structures use MSA as inputs, which is a huge restriction. Indeed, significant families are still unknown (32). It also increases the inference time, where a homology search should be made for each prediction. Our method leverages language model without the need of homology, which is a benefit for the prediction of RNA from unknown families.

Through the evaluation of our model for backbone torsional angles prediction, we have extended this evaluation as a model quality assessment for RNA 3D structures. Then, we have inferred a scoring function named RNA-Torsion-A. This scoring function could help the selection of near-native structures in terms of angle deviation. It is also specific to torsional angles and, thus, is more related to the MCQ (mean of circular quantities) than the other atom-deviation-based metrics. RNA-Torsion-A is, therefore, the best scoring function to reproduce the MCQ metric.

Improvements could be made for both RNA-TorsionBERT and RNA-Torsion-A. The RNA-TorsionBERT performances remain limited to reconstruct the structures from just the torsional angles. Indeed, the reconstruction from torsional angles alone is difficult as small angle deviation could lead to high cumulative divergence. The number of solved structures remain the main bottleneck to train robust methods. The quality of the scoring function could be enhanced by incorporating distance atom features, or directly by improving the prediction of torsional angles itself.

Our RNA-TorsionBERT method can nonetheless be used as a starting point for the reconstruction of RNA 3D structures, with *ab initio* methods, for instance, that include molecular dynamics to relax the structure. It could also be used as a feature in a bigger network to predict RNA 3D conformation. Sugar conformation could also be added to improve the structural features predicted.

ACKNOWLEDGEMENTS
This work is supported in part by UDOPIA-ANR-20-THIA-0013, Labex DigiCosme (project

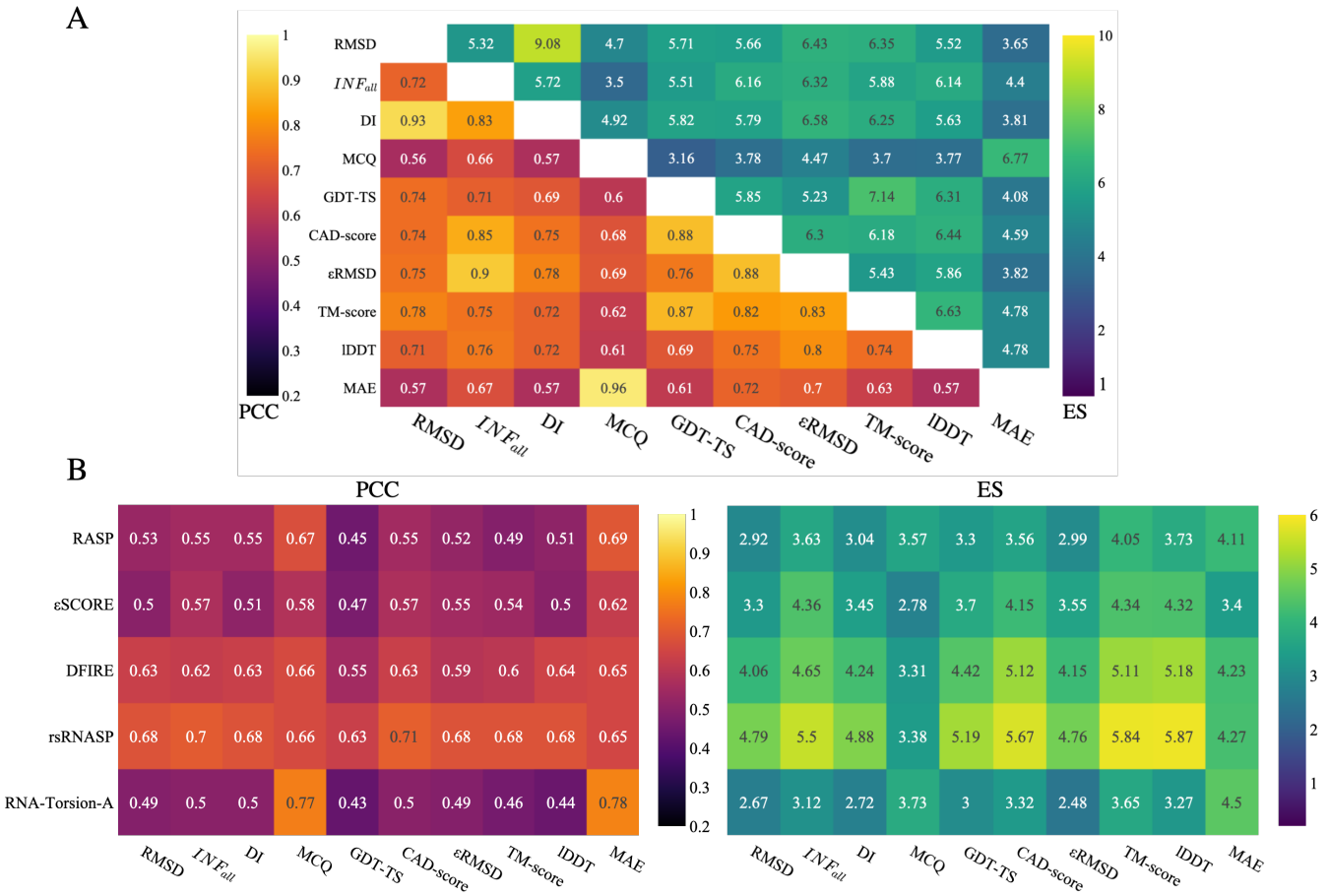

Figure 6. Correlation in terms of PCC and ES between metrics and scoring functions averaged over the three Decoy sets. The lighter the colour, the better the correlation. A) PCC (lower half) and ES (upper half) for ten metrics (RMSD, INF_{all} (53), DI (53), MCQ (54), GDT-TS (50), CAD-score (52), ϵRMSD (25), TM-score (56), lDDT (51) and MAE). The diagonal has a PCC of 1 and ES of 10. B) PCC (left) and ES (right) between five different scoring functions (RASP (20), ϵSCORE (25), DFIRE-RNA (21), rsRNASP (22) and our RNA-Torsion-A scoring function) and ten metrics.

ANR11LABEX0045DIGICOSME), performed using HPC resources from GENCI/IDRIS (grant AD011014250), and operated by ANR as part of the program "Investissement d'Avenir" Idex ParisSaclay (ANR11IDEX000302).
Conflict of Interest: None is declared.

Bibliography

1. Kailong Zhang, Shuai Li, Kristina Kappel, et al. Cryo-EM structure of a 40 kDa SAM-IV riboswitch RNA at 3.7 Å resolution. *Nature Communications*, 10:5511, 2019.
2. Clément Bernard, Guillaume Postic, Sahar Ghannay, and Fariza Tahi. State-of-the-RNArt: benchmarking current methods for RNA 3D structure prediction. *NAR Genomics and Bioinformatics*, 6(2):lqae048, June 2024. doi: 10.1093/nargab/lqae048.
3. John Jumper, Richard Evans, Alexander Pritzel, et al. Highly accurate protein structure prediction with AlphaFold. *Nature*, 596:583–589, 8 2021.
4. R Das, RC Kretsch, AJ Simpkin, et al. Assessment of three-dimensional RNA structure prediction in CASP15. *Proteins*, 91(12):1747–1770, 2023.
5. Bohdan Schneider, Blake Alexander Sweeney, Alex Bateman, Jiri Cerny, Tomasz Zok, and Marta Szachniuk. When will RNA get its AlphaFold moment? *Nucleic Acids Research*, 51 (18):9522–9532, 2023. doi: 10.1093/nar/gkad726.
6. J. Abramson, J. Adler, J. Dunger, et al. Accurate structure prediction of biomolecular interactions with AlphaFold 3. *Nature*, 2024. doi: 10.1038/s41586-024-07487-w.
7. Clément Bernard, Guillaume Postic, Sahar Ghannay, and Fariza Tahi. Has alphafold 3 reached its success for rnas? *bioRxiv*, 6 2024. doi: 10.1101/2024.06.13.598780.
8. Neocles B. Leontis and Eric Westhof. Geometric nomenclature and classification of RNA base pairs. *RNA*, 7(4):499–512, April 2001. doi: 10.1017/s1355838201002515.
9. Bohdan Schneider, Zdenek Moravek, and Helen M. Berman. RNA conformational classes. *Nucleic Acids Research*, 32(5):1666–1677, March 2004. doi: 10.1093/nar/gkh333.
10. L. J. Murray, III Arendall, W. B., D. C. Richardson, and J. S. Richardson. RNA backbone is rotameric. *Proceedings of the National Academy of Sciences of the United States of America*, 100(24):13904–13909, 2003. doi: 10.1073/pnas.1835769100.
11. Lisa M Wadley, Kevin S Keating, Carlos M Duarte, and Anna Marie Pyle. Evaluating and learning from RNA pseudotorsional space: quantitative validation of a reduced representation for RNA structure. *J Mol Biol*, 372(4):942–957, Sep 2007. ISSN 0022-2836. doi: 10.1016/j.jmb.2007.06.058.
12. J. Parsons, J. B. Holmes, J. M. Rojas, J. Tsai, and C. E. Strauss. Practical conversion from torsion space to Cartesian space for in silico protein synthesis. *Journal of Computational Chemistry*, 26(10):1063–1068, July 2005. doi: 10.1002/jcc.20237.
13. E. Alcaide, S. Biderman, A. Telenti, and M. C. Maher. MP-NeRF: A massively parallel method for accelerating protein structure reconstruction from internal coordinates. *Journal of Computational Chemistry*, 43(1):74–78, January 2022. doi: 10.1002/jcc.26768. Epub 2021 Oct 28.
14. Jaswinder Singh, Kuldip Paliwal, Jaspreet Singh, et al. RNA Backbone Torsion and Pseudo-torsion Angle Prediction Using Dilated Convolutional Neural Networks. *Journal of Chemical Information and Modeling*, 61:2610–2622, 6 2021.
15. Jacob Devlin, Ming-Wei Chang, Kenton Lee, and Kristina Toutanova. BERT: pre-training of deep bidirectional transformers for language understanding. *CoRR*, abs/1810.04805, 2018.
16. Manato Akiyama and Yasubumi Sakakibara. Informative RNA base embedding for RNA structural alignment and clustering by deep representation learning. *NAR Genomics and Bioinformatics*, 4(1):lqac012, 02 2022.
17. Yanrong Ji, Zhihan Zhou, Han Liu, et al. DNABERT: pre-trained Bidirectional Encoder Representations from Transformers model for DNA-language in genome. *Bioinformatics*, 37: 2112–2120, 8 2021.
18. Zhihan Zhou, Yanrong Ji, Weijian Li, et al. DNABERT-2: Efficient Foundation Model and Benchmark For Multi-Species Genome, 2023.
19. Jian Wang, Yunjie Zhao, Chunyan Zhu, et al. 3dRNAscore: a distance and torsion angle dependent evaluation function of 3D RNA structures. *Nucleic Acids Research*, 43:e63–e63, 5 2015.
20. Emidio Capriotti, Tomas Norambuena, Marc A. Marti-Renom, et al. All-atom knowledge-based potential for RNA structure prediction and assessment. *Bioinformatics*, 27:1086–1093, 4 2011.
21. Emidio Capriotti, Tomas Norambuena, Marc A. Marti-Renom, et al. All-atom knowledge-based potential for RNA structure prediction and assessment. *Bioinformatics*, 27(8):1086–1093, 02 2011.
22. Ya-Lan Tan, Xunxun Wang, Ya-Zhou Shi, et al. rsRNASP: A residue-separation-based statistical potential for RNA 3D structure evaluation. *Biophysical Journal*, 121:142–156, 1 2022.
23. Jun Li, Wei Zhu, Jun Wang, et al. RNA3DCNN: Local and global quality assessments of RNA 3D structures using 3D deep convolutional neural networks. *PLOS Computational*

Biology, 14(11):1–18, 11 2018.
24. Raphael J. L. Townshend, Stephan Eismann, Andrew M. Watkins, et al. Geometric deep learning of RNA structure. *Science*, 373:1047–1051, 8 2021.
25. Sandro Bottaro, Francesco Di Palma, and Giovanni Bussi. The Role of Nucleobase Interactions in RNA Structure and Dynamics. *Nucleic acids research*, 42, 10 2014.
26. K. Sato, M. Akiyama, and Y. Sakakibara. RNA secondary structure prediction using deep learning with thermodynamic integration. *Nature Communications*, 12(1):941, 2021. doi: 10.1038/s41467-021-21194-4.
27. Laiyi Fu, Yingxin Cao, Jie Wu, Qinke Peng, Qing Nie, and Xiaohui Xie. UFold: fast and accurate RNA secondary structure prediction with deep learning. *Nucleic Acids Research*, 50(3):e14, February 2022. doi: 10.1093/nar/gkab1074.
28. Ashish Vaswani, Noam Shazeer, Niki Parmar, et al. Attention is All you Need. In *Advances in Neural Information Processing Systems*, volume 30. Curran Associates, Inc., 2017.
29. Jiayang Chen, Zhihang Hu, Siqi Sun, Qingxiong Tan, Yixuan Wang, Qinze Yu, Licheng Zong, Liang Hong, Jin Xiao, Tao Shen, Irwin King, and Yu Li. Interpretable RNA Foundation Model from Unannotated Data for Highly Accurate RNA Structure and Function Predictions. 2022.
30. Xi Wang, Ruichu Gu, Zhiyuan Chen, Yongge Li, Xiaohong Ji, Guolin Ke, and Han Wen. UNI-RNA: UNIVERSAL PRE-TRAINED MODELS REVOLUTIONIZE RNA RESEARCH. *bioRxiv*, 2023. doi: 10.1101/2023.07.11.548588.
31. Yikun Zhang, Mei Lang, Jiuhong Jiang, Zhiqiang Gao, Fan Xu, Thomas Litfin, Ke Chen, Jaswinder Singh, Xiansong Huang, Guoli Song, Yonghong Tian, Jian Zhan, Jie Chen, and Yaoqi Zhou. Multiple sequence alignment-based RNA language model and its application to structural inference. *Nucleic Acids Research*, 52(1):e3, 2024. doi: 10.1093/nar/gkad1031.
32. Ioanna Kalvari, Joanna Argasinska, Natalia Quinones-Olvera, et al. Rfam 13.0: Shifting to a genome-centric resource for non-coding RNA families. *Nucleic Acids Res.*, 46:D335–D342, 2018.
33. Andrew Colasanti, Xiang-Jun Lu, and Wilma K. Olson. Analyzing and building nucleic acid structures with 3DNA. *Journal of Visualized Experiments*, 74:e4401, 2013.
34. José Almeida Cruz, Marc-Frédérick Blanchet, Michal Boniecki, Janusz M. Bujnicki, Shi-Jie Chen, Song Cao, Rhiju Das, Feng Ding, Nikolay V. Dokholyan, Samuel Coulbourn Flores, Lili Huang, Christopher A. Lavender, Véronique Lisi, François Major, Katarzyna Mikolajczak, Dinshaw J. Patel, Anna Philips, Tomasz Puton, John Santalucia, Fredrick Sijenyi, Thomas Hermann, Kristian Rother, Magdalena Rother, Alexander Serganov, Marcin Skorupski, Tomasz Soltysinski, Parin Sripakdeevong, Irina Tuszynska, Kevin M. Weeks, Christina Waldsich, Michael Wildauer, Neocles B. Leontis, and Eric Westhof. Rna-puzzles : A casp-like evaluation of rna three-dimensional structure prediction. *RNA*, 18:610–625, 4 2012. ISSN 1355-8382. doi: 10.1261/rna.031054.111.
35. Zhichao Miao, Ryszard W Adamiak, Marc F Blanchet, Michal Boniecki, Janusz M Bujnicki, Shi-Jie Chen, Clarence Cheng, Grzegorz Chojnowski, Fang-Chieh Chou, Pablo Cordero, Jose Almeida Cruz, Adrian R Ferré-D'Amaré, Rhiju Das, Feng Ding, Nikolay V Dokholyan, Stanislaw Dunin-Horkawicz, Wipapat Kladwang, Andrey Krokhotin, Grzegorz Lach, Marcin Magnus, and et al. Rna-puzzles round ii: assessment of rna structure prediction programs applied to three large rna structures. *RNA*, 21(6):1066–1084, 2015. doi: 10.1261/rna.049502.114.
36. Zhichao Miao, Ryszard W. Adamiak, Maciej Antczak, Robert T. Batey, Alexander J. Becka, Marcin Biesiada, Michał J. Boniecki, Janusz M. Bujnicki, Shi-Jie Chen, Clarence Yu Cheng, Fang-Chieh Chou, Adrian R. Ferré-D'Amaré, Rhiju Das, Wayne K. Dawson, Feng Ding, Nikolay V. Dokholyan, Stanisław Dunin-Horkawicz, Caleb Geniesse, Kalli Kappel, Wipapat Kladwang, Andrey Krokhotin, Grzegorz E. Łach, François Major, Thomas H. Mann, Marcin Magnus, Katarzyna Pachulska-Wieczorek, Dinshaw J. Patel, Joseph A. Piccirilli, Mariusz Popenda, Katarzyna J. Purzycka, Aiming Ren, Greggory M. Rice, John Santalucia, Joanna Sarzynska, Marta Szachniuk, Arpit Tandon, Jeremiah J. Trausch, Siqi Tian, Jian Wang, Kevin M. Weeks, Benfeard Williams, Yi Xiao, Xiaojun Xu, Dong Zhang, Tomasz Zok, and Eric Westhof. Rna-puzzles round iii: 3d rna structure prediction of five riboswitches and one ribozyme. *RNA*, 23:655–672, 5 2017. ISSN 1355-8382. doi: 10.1261/rna.060368.116.
37. Zhichao Miao, Ryszard W. Adamiak, Maciej Antczak, Michał J. Boniecki, Janusz Bujnicki, Shi-Jie Chen, Clarence Yu Cheng, Yi Cheng, Fang-Chieh Chou, Rhiju Das, Nikolay V. Dokholyan, Feng Ding, Caleb Geniesse, Yangwei Jiang, Astha Joshi, Andrey Krokhotin, Marcin Magnus, Olivier Mailhot, Francois Major, Thomas H. Mann, Paweł Piątkowski, Radoslaw Pluta, Mariusz Popenda, Joanna Sarzynska, Lizhen Sun, Marta Szachniuk, Siqi Tian, Jian Wang, Jun Wang, Andrew M. Watkins, Jakub Wiedemann, Yi Xiao, Xiaojun Xu, Joseph D. Yesselman, Dong Zhang, Yi Zhang, Zhenzhen Zhang, Chenhan Zhao, Peinan Zhao, Yuanzhe Zhou, Tomasz Zok, Adriana Żyła, Aiming Ren, Robert T. Batey, Barbara L. Golden, Lin Huang, David M. Lilley, Yijin Liu, Dinshaw J. Patel, and Eric Westhof. Rna-puzzles round iv: 3d structure predictions of four ribozymes and two aptamers. *RNA*, 26: 982–995, 8 2020. ISSN 1355-8382. doi: 10.1261/rna.075341.120.
38. Dong Zhang, Jun Li, and Shi-Jie Chen. IsRNA1: De Novo Prediction and Blind Screening of RNA 3D Structures. *Journal of Chemical Theory and Computation*, 17:1842–1857, 3 2021.
39. Jun Li and Shi-Jie Chen. RNAJP: enhanced RNA 3D structure predictions with non-canonical interactions and global topology sampling. *Nucleic Acids Research*, 51:3341–3356, 4 2023.
40. Jiajie Li, Shanshan Zhang, Dan Zhang, et al. Vfold-Pipeline: a web server for RNA 3D structure prediction from sequences. *Bioinformatics*, 38(16):4042–4043, 2022.
41. Mariusz Popenda, Marta Szachniuk, Maciej Antczak, et al. Automated 3D structure composition for large RNAs. *Nucleic Acids Research*, 40:e112–e112, 8 2012.
42. Marc Parisien and François Major. The MC-Fold and MC-Sym pipeline infers RNA structure from sequence data. *Nature*, 452:51–55, 3 2008.
43. Jun Wang, Jian Wang, Yanzhao Huang, et al. 3dRNA v2.0: An Updated Web Server for RNA 3D Structure Prediction. *International Journal of Molecular Sciences*, 20:4116, 8 2019.
44. W. Wang, C. Feng, R. Han, et al. trRosettaRNA: automated prediction of RNA 3D structure with transformer network. *Nat Commun*, 14:7266, 2023.
45. Tao Shen, Zhihang Hu, Zhangzhi Peng, et al. E2Efold-3D: End-to-End Deep Learning Method for Accurate de Novo RNA 3D Structure Prediction. *arXiv preprint arXiv:2207.01586*, 2022.
46. Andrew Martin Watkins, Ramya Rangan, and Rhiju Das. FARFAR2: Improved De Novo Rosetta Prediction of Complex Global RNA Folds. *Structure*, 28:963–976.e6, 8 2020.
47. Michal J. Boniecki, Grzegorz Lach, Wayne K. Dawson, et al. SimRNA: a coarse-grained method for RNA folding simulations and 3D structure prediction. *Nucleic Acids Research*, 44:e63–e63, 4 2016.
48. Marcin Magnus, Maciej Antczak, Tomasz Zok, et al. RNA-Puzzles toolkit: a computational resource of RNA 3D structure benchmark datasets, structure manipulation, and evaluation tools. *Nucleic Acids Research*, 48(2):576–588, 12 2019.
49. Yang Zhang and Jeffrey Skolnick. Scoring function for automated assessment of protein structure template quality. *Proteins*, 57(4):702—710, December 2004.
50. Adam Zemla, Ceslovas Venclovas, John Moult, et al. Processing and analysis of CASP3 protein structure predictions. *Proteins: Structure, Function, and Bioinformatics*, 37(S3): 22–29, 1999.
51. Valerio Mariani, Marco Biasini, Alessandro Barbato, et al. lDDT: a local superposition-free score for comparing protein structures and models using distance difference tests. *Bioinformatics (Oxford, England)*, 29(21):2722–2728, 2013.
52. Kliment Olechnovic, Eleonora Kulberkyte, and Ceslovas Venclovas. CAD-score: A new contact area difference-based function for evaluation of protein structural models. *Proteins*, 81, 01 2013.
53. Marc Parisien, José Cruz, Eric Westhof, et al. New metrics for comparing and assessing discrepancies between RNA 3D structures and models. *RNA (New York, N.Y.)*, 15:1875–85, 09 2009.
54. Tomasz Zok, Mariusz Popenda, and Marta Szachniuk. MCQ4Structures to compute similarity of molecule structures. *Central European Journal of Operations Research*, 22, 04 2013.
55. Clement Bernard, Guillaume Postic, Sahar Ghannay, and Fariza Tahi. RNAdvisor: a comprehensive benchmarking tool for the measure and prediction of RNA structural model quality. *Briefings in Bioinformatics*, 25:bbae064, March 2024.
56. Chengxin Zhang, Morgan Shine, Anna Marie Pyle, et al. US-align: Universal Structure Alignment of Proteins, Nucleic Acids and Macromolecular Complexes. *Nature Methods*, 19: 1109–1115, 2022.
57. Robin Pearce, Gilbert S. Omenn, and Yang Zhang. De Novo RNA Tertiary Structure Prediction at Atomic Resolution Using Geometric Potentials from Deep Learning. *bioRxiv*, May 2022.
58. Y. Kagaya, Z. Zhang, N. Ibtehaz, X. Wang, T. Nakamura, D. Huang, and D. Kihara. NuFold: A Novel Tertiary RNA Structure Prediction Method Using Deep Learning with Flexible Nucleobase Center Representation. *bioRxiv*, September 2023. doi: 10.1101/2023.09.20.558715. Preprint.
59. Minkyung Baek, Reid McHugh, Ivan Anishchenko, et al. Accurate prediction of protein–nucleic acid complexes using RoseTTAFoldNA. *Nature Methods*, 21:117–121, 2024. doi: 10.1038/s41592-023-02086-5.
60. Y. Li, C. Zhang, C. Feng, et al. Integrating end-to-end learning with deep geometrical potentials for ab initio RNA structure prediction. *Nature Communications*, 14:5745, 2023.